Received: 18 November 2020 | Accepted: 10 February 2021

DOI: 10.1111/jth.15288

ORIGINAL ARTICLE

Probing activation-driven changes in coagulation factor IX by mass spectrometry

Nadia Freato[1] | Floris P. J. van Alphen[1] | Mariëtte Boon-Spijker[1] | Maartje van den Biggelaar[1] | Alexander B. Meijer[1,2] | Koen Mertens[1,3] | Eduard H. T. M. Ebberink[1]

[1]Department of Molecular and Cellular Hemostasis, Sanquin Research, Amsterdam, The Netherlands

[2]Department of Biomolecular Mass Spectrometry and Proteomics, Utrecht Institute for Pharmaceutical Sciences (UIPS), Utrecht University, Utrecht, The Netherlands

[3]Department of Pharmaceutics, Utrecht Institute for Pharmaceutical Sciences (UIPS), Utrecht University, Utrecht, The Netherlands

Correspondence
Koen Mertens, Department of Molecular and Cellular Hemostasis, Sanquin Research, Plesmanlaan 125, 1066 CX Amsterdam, The Netherlands.
Email: k.mertens@sanquin.nl

Funding information
Utrecht Institute for Pharmaceutical Sciences (UIPS); Landsteiner Stichting voor Bloedtransfusie Research, Grant/Award Number: LSBR 1417

Abstract

Background: Activated factor IX (FIXa) is an inefficient enzyme that needs activated factor VIII (FVIII) for full activity. Recently, we identified a network of FVIII-driven changes in FIXa employing hydrogen-deuterium eXchange mass spectrometry (HDX-MS). Some changes also occurred in active-site inhibited FIXa, but others were not cofactor-driven, in particular those within the 220-loop (in chymotrypsin numbering).

Objective: The aim of this work is to better understand the zymogen-to-enzyme transition in FIX, with specific focus on substrate-driven changes at the catalytic site.

Methods: Footprinting mass spectrometry by HDX and Tandem-Mass Tags (TMT) labelling were used to explore changes occurring upon the conversion from FIX into FIXa. Mutagenesis and kinetic studies served to assess the role of the 220-loop.

Results: HDX-MS displayed remarkably few differences between FIX and FIXa. In comparison with FIX, FIXa did exhibit decreased deuterium uptake at the N-terminus region. This was more prominent when the FIXa active site was occupied by an irreversible inhibitor. TMT-labelling showed that the N-terminus is largely protected from labelling, and that inhibitor binding increases protection to a minor extent. Occupation of the active site also reduced deuterium uptake within the 220-loop backbone. Mutagenesis within the 220-loop revealed that a putative H-bond network contributes to FIXa activity. TMT labeling of the N-terminus suggested that these 220-loop variants are more zymogen-like than wild-type FIXa.

Conclusion: In the absence of cofactor and substrate, FIXa is predominantly zymogen-like. Stabilization in its enzyme-like form involves, apart from FVIII-binding, also interplay between the 220-loop, N-terminus, and the substrate binding site.

KEYWORDS
active site, factor IX, hydrogen-deuterium exchange, mass spectrometry, serine protease, zymogen

Manuscript handled by: Alan Mast

Final decision: Alan Mast, 10 February 2021

Essentials

- Activated Factor IX (FIXa) is a poor enzyme that needs factor VIII-driven stabilization for efficient catalysis.
- Mass spectrometry reveals that the protease domain of FIXa is predominantly zymogen-like.
- The active conformation involves interplay between the 220-loop N-terminus and substrate-binding.
- The full catalytic potential of FIXa requires both cofactor- and substrate-driven structural changes.

1 | INTRODUCTION

Factor IX (FIX) is an essential constituent of the coagulation cascade, which is characterized by the sequential conversion of inactive zymogens into active serine proteases.[1,2] Apart from FIX, other zymogens in the cascade include FVII, FX, and prothrombin. These are the precursors of their active counterparts FIXa, FVIIa, FXa, and thrombin, respectively. As members of the chymotrypsin superfamily of serine proteases, they require limited proteolysis for activation. Proteolysis at the N-terminal region of the catalytic domain exposes a novel N-terminus, which refolds into the protease domain and thereby stabilizes the catalytic site.[3-5] The FIX zymogen circulates as a single-chain molecule. It comprises a γ-carboxyglutamic acid-rich domain (Gla domain) at the N-terminus, followed by two epidermal growth factor (EGF)-like domains (EGF1 and EGF2), a glycosylated activation peptide, and the protease domain at the C-terminus.[6-8] FIX is converted into FIXa by FVIIa or activated factor XI (FXIa).[6] Activation involves the release of the glycosylated activation peptide by two subsequent steps, at Arg145 and Arg180. This results a two-chain molecule, a light chain of amino acids 1 to 145 (the Gla-EGF1-EGF2 section), and a heavy chain of residues 181 to 415. The latter represents the serine protease domain, with Val181{16_{CT}} as the N-terminus (subscript CT denotes chymotrypsin numbering).

As with other serine proteases, the catalytic domain of FIX displays a dual antiparallel β-barrel architecture, in which the interface between the β-barrel domains encloses the catalytic center and the substrate recognition pockets.[3,5] Apart from these common structural elements, the β-barrels carry eight surface loops that are variable between individual serine proteases. These loops provide insertions that protrude from the protein core, and support unique, protease-specific interactions, or more general allosteric events.[9] The latter includes the 70-$loop_{CT}$, which provides a Ca^{2+}-binding site that plays an allosteric role in FVIIa, FIXa, and FXa.[10-12] Similarly, the 220-$loop_{CT}$, together with the 180-$loop_{CT}$, comprises a Na^{+}-binding site that contributes to the catalytic activity of thrombin, FXa, and, to a lesser extent, of FIXa.[13-15] More specific allosteric changes in these proteases are driven by assembly with their natural cofactors, such as in the tissue factor (TF)-FVIIa complex, and in the complex of FIXa with activated factor VIII (FVIIIa).[16,17]

It has been well established that FIXa displays low intrinsic activity, and needs assembly with its cofactor FVIIIa on phospholipid membranes to develop its full enzymatic potential.[18,19] Obviously, the generation of the novel N-terminus, and the putative insertion thereof into the catalytic site, is insufficient to fully activate FIX. Although in chymotrypsin limited proteolysis alone seems sufficient to drive the protease domain into the fully active state, the coagulation proteases display a more complex zymogen to protease transition.[20-22] Structural information and rapid kinetics have established that thrombin, despite being fully activated in terms of proteolytic processing, can adopt both protease-like and zymogen-like forms, which are in dynamic equilibrium. This includes the distinction between "fast" and "slow" thrombin, or in more general terms, between zymogen-like enzymes and enzyme-like zymogens.[23] As for the zymogen/enzyme pair FVII/FVIIa, hydrogen/deuterium exchange mass spectrometry (HDX-MS) studies have demonstrated that FVII and FVIIa share the same solution structure, whereas the transition of FVIIa into a protease-like conformation is driven either by assembly with its cofactor TF, or by the incorporation of an irreversible inhibitor into the active site.[16] This raises the question as to whether FIXa, despite being proteolytically activated, could be predominantly zymogen-like, thus explaining its low enzymatic activity.

We recently explored FVIII-driven changes in FIXa by HDX-MS, and observed a variety of allosteric changes, suggesting an overall rigidification of the FIXa catalytic domain upon FVIIIa binding.[17] Cofactor-induced changes proved to overlap partially with those because of the occupation of the substrate-binding site by an active site-directed inhibitor. Moreover, occupation of the S1 pocket, but not cofactor binding, induced changes in the 220-$loop_{CT}$, reflecting a specific linkage between this loop and maturation of the active site.[15,17] Although this implies that FIXa requires both active site occupation and cofactor binding to develop its full catalytic potential, it remains unclear to what extent free FIXa is enzyme or zymogen like. In the present paper, we address this question by comparing the FIX zymogen, FIXa, and inhibitor-bound FIXa, with particular reference to the interplay between the 220-$loop_{CT}$ and the N-terminus Val181{16_{CT}} of the protease domain. Employing HDX-MS combined with tandem-mass tag (TMT) studies, site-directed mutagenesis, and functional analysis, we observed that FIXa is predominantly zymogen-like, but does display a few enzyme-like properties that are inherent to its proteolytic activation.

2 | MATERIALS AND METHODS

2.1 | Materials

Chromogenic substrate CH_3SO_2-(D)-CHG-Gly-Arg-*p*Na (Pefachrome FIXa) was obtained from Pentapharm and S-2765 containing the thrombin inhibitor I-2581 was from Chromogenix. H-Glu-Gly-Arg-chloromethylketone (EGRck) was from Bachem. Calcium chloride 1 M solution and deuterium oxide 99.9% were from Sigma-Aldrich. Ultrapure urea, Molecular Biology grade 5 M NaCl solution, and Tris-HCl were from Invitrogen. Chicken egg L-α-phosphatidylcholine (PC) and porcine brain L-α-phosphatidylserine were from Avanti Polar Lipids Inc. *N*-2 hydroxyethylpiperazine-N'-ethanesulfonic acid (HEPES) was from Serva. Tris(2-carboxyethyl) phosphine hydrochloride, the TMTduplex Isobaric Tagging kit, Zeba Spin columns (7 K, 0.5 mL), and chymotrypsin were from Thermo Scientific. All other chemicals were from Merck (Darmstadt, Germany).

Images of crystal structures were processed in PyMol v2.4 supplied by Schrödinger. Peaks 7.0 software was used for peptide identification was from Bioinformatics Solution Inc. Deuteration level percentages were calculated using HDeXaminer 2.2.0 software (Sierra Analytics).

2.2 | Proteins used in this study

FIX variants with amino acid substitutions E387A{217_{CT}}, E388A{219_{CT}}, or K394A{224_{CT}} were constructed by site directed mutagenesis in a pcDNA3.1(-) vector encoding wild-type FIX.[24] Mutagenesis was performed using the QuikChange kit (Agilent Technologies, Amstelveen, the Netherlands) using appropriate primers. Mutagenesis was verified by sequencing of the FIX encoding parts on the mutant plasmids. Transfection of HEK293 cells and production of recombinant FIX variants were performed essentially as described elsewhere.[24] Immunopurification using a monoclonal antibody directed against the Gla domain (CLB-FIX 11),[25] subsequent activation, and quantification of recombinant FIX variants have been described elsewhere.[24,26] Human plasma-derived FIX was obtained as immunopurified concentrate (Nonafact, Sanquin Plasma Products), which was further processed by hydrophobic interaction chromatography (Toyopearl-Phenyl 650 M, Tosoh Bioscience) and concentrated by anion exchange chromatography (Q-Sepharose, GE Healthcare, Eindhoven, the Netherlands). Plasma-derived FIX was activated using FXIa. FIXa was purified from the activation mixture, and quantified by active-site titration as described.[26] Active site-inhibited FIXa (FIXaEGR) was prepared by incubation of plasma-derived FIXa (66.5 μM) with EGRck (4 mM) for 45 min at 37°C. Excess of EGRck was removed by anion exchange chromatography employing Q-Sepharose as outlined previously.[24] FIXaEGR was quantified by the Bradford method.[27] Purified FIX and recombinant FIX variants were stored in 20 mM HEPES (pH 7.4) 150 mM NaCl at −30°C. FIXa, FIXaEGR, and FIXa variants were stored at −20°C in a buffer containing 20 mM HEPES (pH 7.4), 150 mM NaCl and 50% (v/v) glycerol.

B-domain-deleted recombinant FVIII was purified with VK34 monoclonal antibody[28] and stored at −20°C in 20 mM HEPES (pH 7.4), 800 mM NaCl, 10 mM $CaCl_2$, and 50% (v/v) glycerol. α-thrombin and FX were obtained as described elsewhere.[29-31] FXIa was from Enzyme Research Laboratories and human serum albumin (HSA) from Sanquin Plasma Products.

2.3 | Enzymatic activity of recombinant FIX variants

Activity of wild-type recombinant FIXa, FIXaE387A{217_{CT}}, FIXaE388A{219_{CT}} and FIXaK394A{224_{CT}} (150 nM) toward the substrate CH_3SO_2-(D)-CHG-Gly-Arg-*p*Na (0-5 mM) was assessed in 50 mM Tris (pH 7.4), 100 mM NaCl, 5 mM $CaCl_2$, and 0.2% HSA at 37°C as described.[24] Activity toward FX was determined in presence of phospholipids (50% PS/50% PC vesicles prepared as described[28]) and varying concentrations of FX in a buffer containing 50 mM Tris (pH 7.4), 150 mM NaCl, 10 mM $CaCl_2$, and 0.2% HSA at 37°C. FXa formation was quantified using S-2765/I-2581 as described.[24] Kinetic constants for amidolytic activity and FX activation were calculated using the Michaelis-Menten equation to obtain K_m and k_{cat} values.

2.4 | Hydrogen/deuterium exchange studies

Plasma-derived FIX, FIXa, or FIXa-EGR (0.03 mM) were preincubated in a buffer containing 200 mM Hepes, 1500 mM NaCl, and 50 mM $CaCl_2$ (pH 7.1). Proteins were then diluted 10-fold in D_2O at 24°C and incubated for 10, 50, 100, 500, 10 000, and 50 000 seconds using an automated sampling handling robot (LEAP technologies, Morrisville, NC).[32] HDX was quenched adding an equal volume of 1.25 M tris(2-carboxyethyl)phosphine hydrochloride, 2 M urea (pH 2.5) at 4°C. Further processing of in-line digestion into peptides and liquid chromatography was done at 4°C. Pepsin digestion was performed by passage of the samples over a Poroszyme Immobilized Pepsin Cartridge (Thermo Scientific) using isocratic flow of 0.1% formic acid with 5% acetonitrile at 100 μl/min for 5 min. Generated peptides were collected on an ethyl-bridged hybrid C18 1.7 μm VanGuard precolumn (Waters). Following 30 s of washing, the precolumn was switched in line with a Hypersil GOLD C18 analytic column (3 μm, 1 × 30 mm, Thermo Scientific). Mass spectrometry analysis was performed as described[17] with the exception that peptides were separated using a 12-minute gradient going from 8% to 40% of a mobile phase of 0.1% (v/v) formic acid in 80% (v/v) acetonitrile under a flow of 50 μl/min. Data were analyzed as described previously.[17] Because relative deuterium uptake of individual peptides was compared, no back-exchange correction was performed.

2.5 | Tandem mass tag labelling studies

Primary amine labelling of wild-type FIXa was performed using the TMT-126 reagent, whereas FIXaEGR or recombinant FIXa variants were labelled by the TMT-127 reagent. Protein (0.5 µM) and TMT reagent (2.5 mM) were incubated for 7.5 minutes at 25°C in a buffer containing 20 mM HEPES (pH 7.4), 150 mM NaCl, and 5 mM $CaCl_2$ in a volume of 80 µl. The reaction was quenched by incubation with 1 µl of 50% hydroxylamine for 15 min. For pairwise quantification, FIXa species labelled by TMT-126 and TMT-127 were mixed in a 1:1 molar ratio. Reduction, alkylation, and proteolytic processing into peptides were performed as described elsewhere.[33] To quantify labelling of the N-terminus, peptides were analyzed using MS^3 fragmentation in an Orbitrap Fusion mass spectrometer (Thermo Scientific, Breda, The Netherlands). Peptides were separated by reversed phase liquid chromatography on a C18-column packed in-house with ReproSil-Pur C18-AQ, 1.9-µm resin (Dr. Maisch, Ammerbuch-Entringen, Germany) in a 20-cm fused silica emitter (75-360 µm inner-outer diameter, New Objective, Woburn, MA). Elution was performed by increasing solution B (0.1% formic acid, 80% acetonitrile) from 5% to 30% (22-132 min) and 30% to 60% (132-147 min). Peptides were sprayed into an Orbitrap Fusion mass spectrometer. Data-dependent acquisition was initiated by a full scan in the Orbitrap with 120,000 resolution power, a scan range between 400 and 1500 m/z, 4.0×10^5 ion count target, and maximum injection time of 50 ms. The 10 most intense precursors with a charge state of 2 to 8 were sampled for MS^2. MS^2 scans were attained following collision-induced dissociation at 35% collision energy and detection in the ion-trap comprising a fragment isolation window of 1.6 m/z and 60 ms maximum injection time. The five most intense ions were selected for subsequent MS^3 fragmentation to quantify the TMT labels. MS^3 fragmentation was performed by higher energy collision–induced dissociation at 65% collision energy and a MS^2 isolation width of 2 m/z. The TMT reporter groups were detected in the Orbitrap with 60 000 resolution power.

3 | RESULTS

3.1 | HDX-MS analysis of FIX, FIXa, and FIXaEGR

Initial inspection of our present HDX-MS data set revealed 93% coverage of the FIX protease domain and 16% of the light chain (Figure S1). As observed previously, peptides from the Gla and EGF-1 domains were not recovered because of the posttranslational modifications therein (i.e., γ-carboxylation and glycosylation), and thus remained beyond the scope of the study.[17] Heat maps suggested limited difference between FIX and FIXa, and an overall protection against deuterium incorporation in FIXaEGR (Figure S1). The amendments in the HDX protocol, compared with our previous study,[17] resulted in higher levels of deuterium uptake. This facilitated the comparison between FIX and its activated counterparts in the present study.

Deuterium uptake plots for all individual peptides are given in supporting Figure S2 and a selection thereof is shown in Figure 1. In comparison with FIXa, FIXaEGR displayed reduced deuterium incorporation in the same peptides as in our previous study,[17] including the 70-$loop_{CT}$, 140-$loop_{CT}$, and 180-$loop_{CT}$ (Figure 1A,C,E). Also, the typical increase in deuterium incorporation in the 99-$loop_{CT}$ was apparent, in particular in the initial time points (Figure 1B). In contrast to FIXaEGR, FIXa and the FIX zymogen displayed similar deuterium uptake. For the vast majority of peptides, there was no appreciable difference between peptides derived from FIX (black) and those from FIXa (red) because virtually all uptake plots were overlapping (Figure 1B,C,D,E and Figure S2). Exceptions included the EGF-2 domain (Figure 1F), the 70-$loop_{CT}$ (Figure 1A), and the N-terminus region (Figure 1H).

Apart from the FIX-derived peptides that were shared with FIXa and FIXaEGR, some peptides were zymogen-specific and comprised the cleavage sites Arg145-Glu146 and Arg180-Val181{16_{CT}} (Figure S3). These peptides displayed a deuterium uptake of 5 Da and more, which was higher than for most of the other peptides (Figure 1). The enhanced deuterium uptake seems compatible with these cleavage sites being flexible and accessible for proteolysis. Peptides containing Val181{16_{CT}} were of particular interest, because they were overlapping with the N-terminal peptide Val181{16_{CT}}-Gln195{30_{CT}} that was derived from FIXa and FIXaEGR (Figure 1G). Although it remains difficult to compare peptides that are not fully identical, the deuterium uptake for the closest matching peptide Thr179-Gln195{30_{CT}} proved strikingly higher than its counterpart, which was truncated by two amino acids because of proteolytic activation (dashed black line in Figure 1G). This suggests that the Val181{16_{CT}}-containing region loses flexibility upon activation, and is further rigidified by EGR incorporation into the active site (Figure 1G). Similar differences, although much less prominent, were observed in the peptide Asp186{21_{CT}}-Leu198{33_{CT}} (Figure 1H). This suggests that the changes observed in the N-terminal region are mainly from the few amino acids surrounding the Arg180-Val181{16_{CT}} scissile bond.

3.2 | Tandem mass tag labelling of the N-terminal region

The changes at the N-terminus of the protease domain (Figure 1G) could reflect the insertion of the newly generated N-terminus into the protease domain, in particular in FIXaEGR. Because HDX accounts for backbone amide changes but not for exposure of primary amines such Lys side chains and the N-terminus, we used TMT labelling to address this issue. Control experiments (data not shown) demonstrated that the labelling protocol resulted in >90% labelling of surface-exposed Lys side chains such as Lys265{98_{CT}}, Lys316{148_{CT}}, and Lys400{230_{CT}}. As for the N-terminal peptide

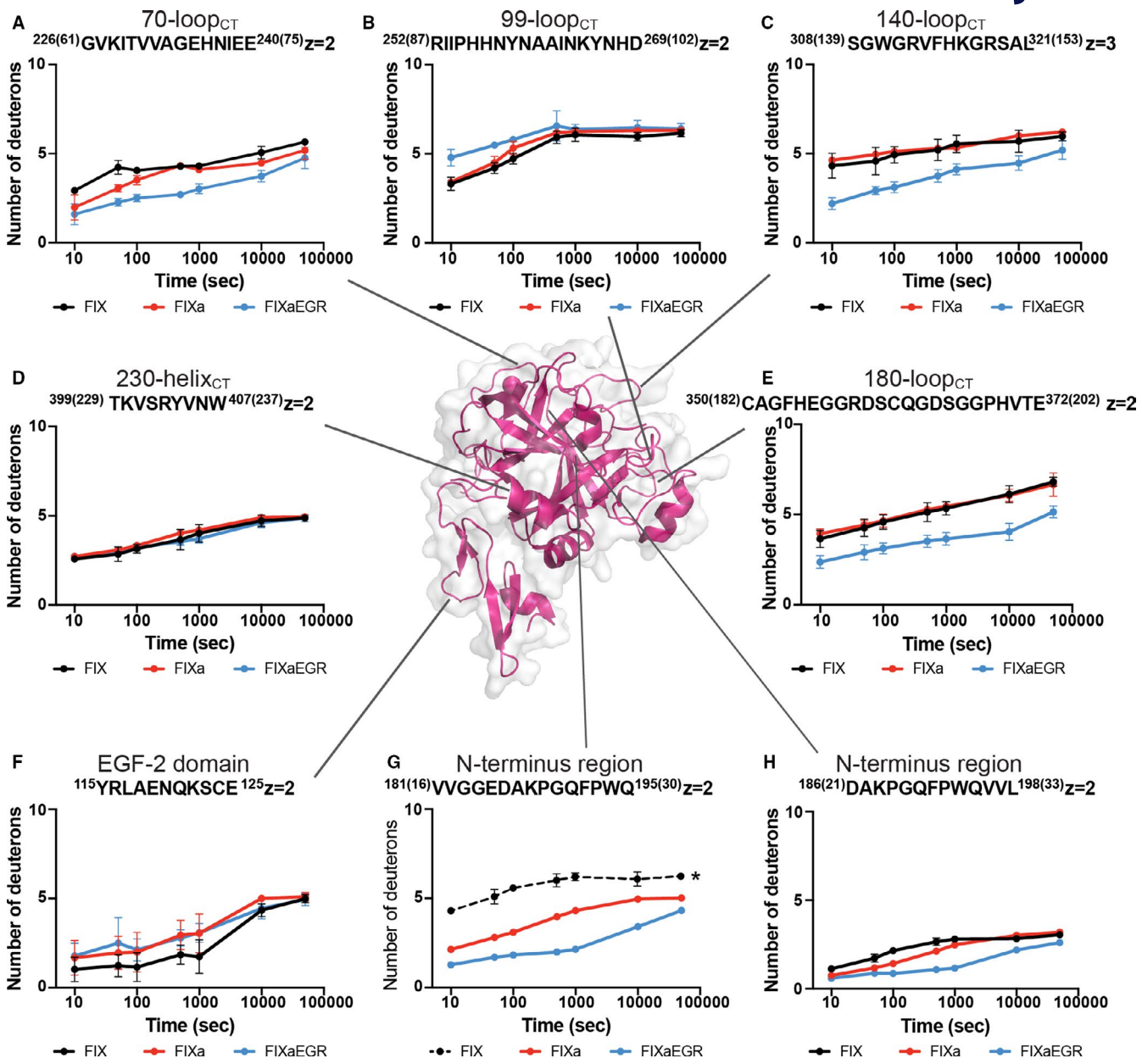

FIGURE 1 HDX-MS of FIX, FIXa, and FIXaEGR. (A-H) Examples of hydrogen-deuterium eXchange (HDX) plots. The peptide sequence is indicated on top of each graph with FIX numbering of the first and last residue. Chymotrypsin numbering is indicated between brackets. Each region is indicated on the crystal structure (PDB code 2wpm[50]). HDX was performed for seven time points (from 10 to 50,000 seconds) as described in Materials and Methods. FIX uptake curves are indicated in black, FIXa is indicated in red, whereas FIXaEGR is shown in blue. Error bars represent the standard deviation of two to six independent measurements. The dashed black curve marked with the asterisk in panel G represents the FIX-unique peptide TRVVGGEDAKPGQFPWQ for comparison with the N-terminal peptide VVGGEDAKPGQFPWQ, which is present in FIXa and FIXaEGR, but not in FIX. See Figure S2 for the full set of peptides and Figure S3 for FIX unique uptake plots [Color figure can be viewed at wileyonlinelibrary.com]

VVGGEDAKPGQFPW, derivatives with and without TMT labels on Val181{16_{CT}} and/or Lys188{23_{CT}} were identified and m/z values of these peptide derivatives were used to reconstruct ion chromatograms. As shown in Figure 2A, these resolved four distinct derivatives, which were unlabeled (red peak), labelled on Lys188{23_{CT}} only (orange), on Val181{16_{CT}} only (black), and labelled in both positions (green). The intensity of these peaks suggested that approximately 80% of the recovered N-terminal peptides did not bear a modified N-terminus, whereas approximately 20% did carry a TMT modification at Val181{16_{CT}}. This suggests that a predominant fraction of the N-terminus in FIXa is protected from labelling by the TMT reagent.

The ion chromatogram shown in Figure 2A is derived from an equimolar mixture of FIXa and FIXaEGR, where each was separately labelled by a different TMT label (see Methods section). This allowed for the quantitative comparison between FIXa and FIXaEGR

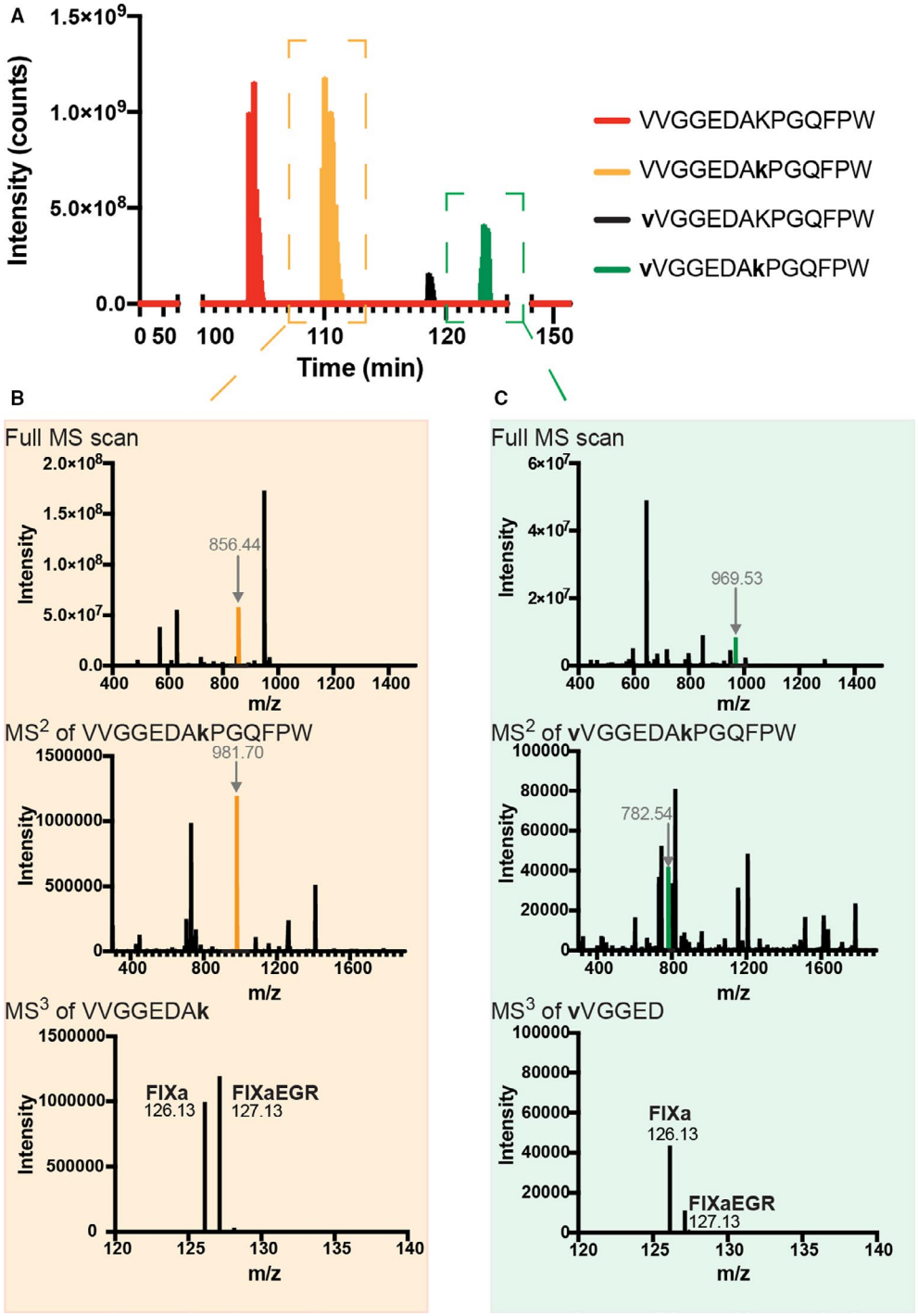

FIGURE 2 Inspection of the N-terminal fragment of the protease domain of FIX. (A) TMT labelling of the N-terminus of FIXa and FIXaEGR. N-terminal peptide VVGGEDAKPGQFPW derivatives with and without TMT labels on $Val16_{CT}$ and/or $Lys23_{CT}$ were identified using Peaks software; m/z values of these peptides were used to extract reconstructed ion chromatograms (RICs). RICs were extracted for N-terminal ions VVGGEDAKPGQFPW (red), VVGGEDA**k**PGQFPW (orange), **v**VGGEDAKPGQFPW (black), and **v**VGGEDA**k**PGQFPW (green). Small and bold **v** and **k** represent modified V and K residues carrying a tandem mass tag. Peptides were identified from MS^2 and abundance percentages were estimated by the highest intensity values. (B) VVGGEDA**k**PGQFPW peptide (m/z 856.44) was fragmented by CID; subsequently, the b8 ion containing the TMT-labelled Lys23 (m/z 981.70) was subjected to MS^3 by HCD to obtain the TMT intensities 126.13 and 127.13. (C) The double labelled **v**VGGEDA**k**PGQFPW peptide (m/z 969.53) was fragmented by CID; subsequently, the b6 ion (m/z 782.54) containing only the TMT-labelled N-terminus (Val16) was subjected to MS^3 by HCD to obtain the TMT intensities 126.13 and 127.13. [Color figure can be viewed at wileyonlinelibrary.com]

by MS^2 and MS^3 fragmentation (Figure 2B,C). In the fraction labelled on Lys188{23_{CT}} only (orange), the intensity for FIXa and FIXaEGR was similar (Figure 2B). In contrast, the fraction labelled in both positions (green), labelling of Val181{16_{CT}} proved approximately fourfold less intense in FIXaEGR (Figure 2C). These data suggest that the N-terminus of the FIXa protease domain is largely protected in FIXaEGR, but also, although to a lesser extent, in noninhibited FIXa.

3.3 | HDX-MS analysis of the 220-loop$_{CT}$

We previously identified the 220-loop$_{CT}$ as a section that displays protection against deuterium exchange upon active site occupation by EGR, but not by assembly with FVIIIa.[17] We therefore addressed the question whether this loop, being located at the edge of the activation pocket in FIXa[7,8] displays any changes upon zymogen activation. Interestingly however, no appreciable difference between FIX and FIXa occurred in this region (Figure 3C-F). One peptide (Figure 3B), showed slightly different time courses, but because of experimental variability, these were considered as overlapping. As anticipated, FIXaEGR displayed reduced deuterium uptake in this region. This was particularly prominent in peptides spanning residues 209-219_{CT} and 220-228_{CT} (Figure 3B,C), and decreased upon extension toward the C-terminus (Figure 3E,F). This pinpoints the protection against deuterium uptake in FIXaEGR to the 220-loop$_{CT}$ and its immediately preceding β-sheet (Figure 3A). Apparently, filling the substrate binding pocket with EGR strongly reduces the flexibility of this part of the protein backbone, whereas noninhibited FIXa remains indistinguishable from the FIX zymogen in this section.

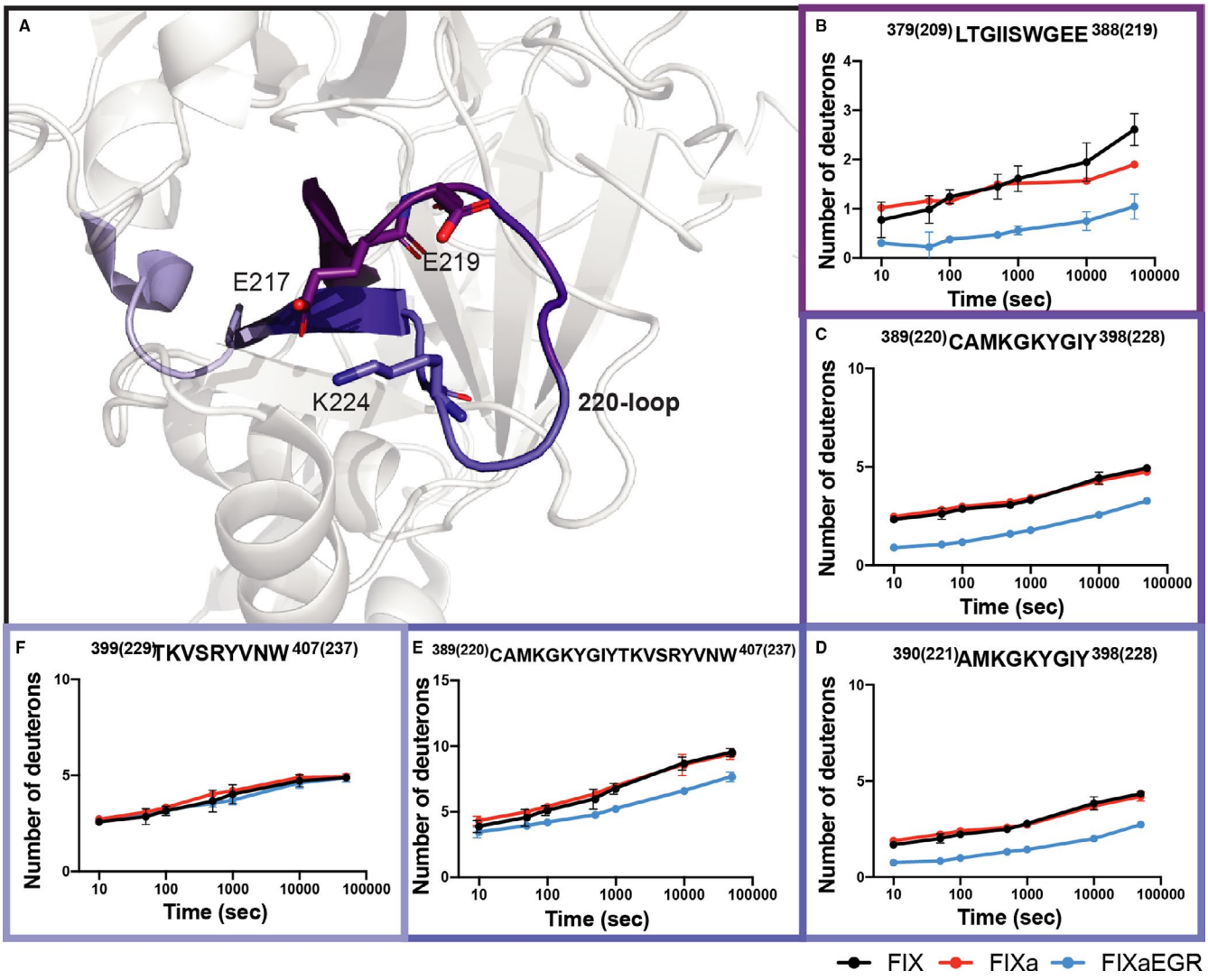

FIGURE 3 HDX-MS plots of FIX, FIXa, and FIXaEGR 220-loop$_{CT}$. (A) The 220-loop$_{CT}$ region is highlighted in color gradient on the FIXa crystal structure (PDB code 2wpm[50]). Charged residues $E217_{CT}$, $E219_{CT}$, and $K224_{CT}$ are displayed in sticks representation. (B-F) HDX-MS plots of the 220-loop$_{CT}$ region are shown with FIX uptake curves indicated in black, FIXa in red, and FIXaEGR in blue. Peptides are mapped in color gradient in panel A [Color figure can be viewed at wileyonlinelibrary.com]

3.4 | Characterization of 220-loop$_{CT}$ variants

With regard to the 209-228$_{CT}$ segment, it is interesting to note that this region has previously been observed to be affected by FIX zymogen to enzyme conversion.[15] It further comprises a H-bond network wherein the side chain of Lys394{224$_{CT}$} contacts the carboxylate groups of E387{217$_{CT}$} and E388{219$_{CT}$}[15] (see Figure 3A). To assess the role of this putative stabilizing network, we produced the recombinant FIXa variants FIXaE387A{217$_{CT}$}, FIXaE388A{219$_{CT}$}, and FIXaK394A{224$_{CT}$}. All three substitutions had a major detrimental effect on FIXa activity (Figure 4). Residual amidolytic activity toward the synthetic substrate CH_3SO_2-(D)-CHG-Gly-Arg-*p*Na (Table 1) was similar for FIXaE387A{217$_{CT}$} and FIXaK394A{224$_{CT}$}, and was mainly reflected by reduction of k_{cat} (Table 1). For FIXaE388A{219$_{CT}$}, k_{cat} was slightly less affected, but still 5-fold lower compared with that of wild-type FIXa. In the absence of FVIIIa, FX activation by FIXaE387A{217$_{CT}$} and FIXaK394A{224$_{CT}$} again proved equally affected (Figure 4A,B and Table 1). The same was observed in the presence of FVIIIa (Figure 4C,D, Table 1). The FIXaE388A{219$_{CT}$} variant differed from the other two in that its defect was less severe. These data suggest that disruption of the putative H-bond network does reduce enzymatic activity. The observation that FIXaE387A{217$_{CT}$} and FIXaK394A{224$_{CT}$} are virtually indistinguishable seems compatible with disruption of a direct interaction between these residues that greatly contributes to FIXa enzymatic activity.

The prominent reduction of FIXa activity in these molecular variants raises the possibility that destabilization of the 220-loop$_{CT}$ drives the catalytic domain into a more zymogen-like form. This possibility was addressed by the same TMT labelling method as used for comparing FIXa and FIXaEGR (Figure 2). Pairwise comparison of mutant and wild-type FIXa is shown in Figure 5. The reconstructed ion chromatograms (Figure 5A,B,C) show that the N-terminal peptide VVGGEDAKPGQFPW was mainly recovered as nonlabelled (red) or labelled on Lys188{23$_{CT}$} only (orange). The fractions carrying the label on the N-terminus Val181{16$_{CT}$} only (black) or on both Val181{16$_{CT}$} and Lys188{23$_{CT}$} (green in Figure 5A) appeared more abundant than observed for wild-type FIXa (Figure 2), in particular for the variant FIXaK394A{224$_{CT}$}. Because these data represent equimolar mixtures of wild-type and mutant FIXa, it remains difficult to derive quantitative information directly from these chromatograms, however. Therefore, both MS^2 and MS^3 fragmentation were used for further quantification based on the TMT labels. Analysis of the fraction that was labelled on both Val181{16$_{CT}$} and Lys188{23$_{CT}$} (green peaks in Figure 5A) showed that N-terminus labelling in FIXaE387A{217$_{CT}$} and FIXaK394A{224$_{CT}$} was 4- to 8-fold more prominent than in wild-type FIXa, while labelling was slightly reduced in FIXaE388A{219$_{CT}$} (Figure 5B). These data suggest that the 220-loop$_{CT}$ variants are similar to wild-type FIXa in that their N-terminus is largely protected against TMT-labelling. However, the extent of protection is lower in FIXaE387A{217$_{CT}$} and FIXaK394A{224$_{CT}$}, which seems compatible with these variants being more zymogen-like. This was not apparent for FIXaE388A{219$_{CT}$}, which displayed a less severe enzymatic defect than the other two variants (Table 1).

4 | DISCUSSION

During the past 5 decades, numerous studies have advanced our understanding of the zymogen to enzyme transition within the class of chymotrypsin-like serine proteases. In the 1970s, crystallographic studies established that chymotrypsinogen and trypsinogen are very

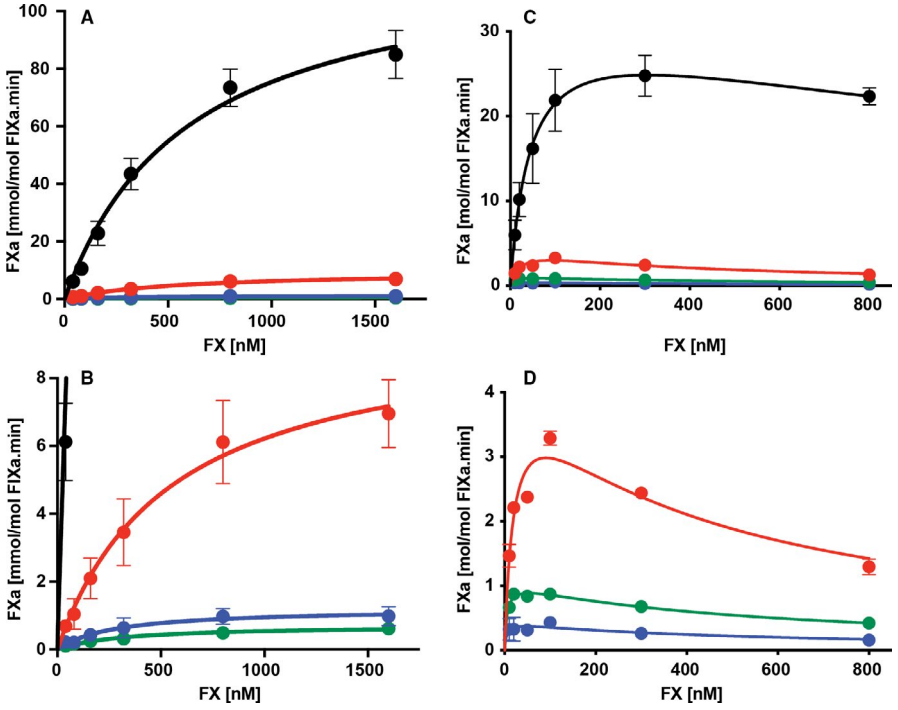

FIGURE 4 Kinetics of FIXa 220-loop variants FIXaE217A$_{CT}$, FIXaE219A$_{CT}$, and FIXaK224A$_{CT}$. (A) FX was converted to FXa in the absence of FVIIIa by 30 nM of wild-type FIXa (black) or FIXa variants FIXaE219A$_{CT}$ (red), FIXaE217A$_{CT}$ (blue), and FIXaK224A$_{CT}$ (green). (B) Zoom of FIXaE219A$_{CT}$ (red), FIXaE217A$_{CT}$ (blue), FIXaK224A$_{CT}$ (green) kinetics in the absence of FVIIIa. (C) FX activation by 0.3 nM of wild-type FIXa (black), FIXaE219A$_{CT}$ (red), FIXaE217A$_{CT}$ (blue), and FIXaK224A$_{CT}$ (green) in presence of FVIIIa (0.35 nM). (D) Close-up of FIXaE219A$_{CT}$ (red), FIXaE217A$_{CT}$ (blue), and FIXaK224A$_{CT}$ (green) kinetics in the presence of FVIIIa. Experimental conditions are described in Materials and Methods [Color figure can be viewed at wileyonlinelibrary.com]

TABLE 1 Kinetic properties of 220-loop$_{CT}$ mutants for cleavage of CH_3SO_2-(D)-CHG-Gly-Arg-*p*Na and the natural substrate FX in absence and presence of FVIIIa

	Amidolytic Activity		FX Activation in Absence of FVIIIa		FX Activation in the Presence of FVIIIa	
	K_m (mM)	k_{cat} (min^{-1})	$K_{m,app}$ (μM)	$10^3 x$ $k_{cat,app}$ (min^{-1})	$K_{m,app}$ (nM)	$k_{cat,app}$ (min^{-1})
FIXa wild-type	2.0 ± 0.3	66.7 ± 4	0.6 ± 0.1	121 ± 8	35 ± 7	28 ± 2
FIXaE217A$_{CT}$	1.6 ± 0.4	5.3 ± 0.6	0.3 ± 0.1	1.2 ± 0.2	ND[a]	0.4 ± 0.1
FIXaE219A$_{CT}$	3.1 ± 0.5	13.3 ± 1	0.6 ± 0.1	10 ± 1	ND[a]	4.2 ± 1.2
FIXaK224A$_{CT}$	2.0 ± 0.7	5.3 ± 0.7	0.3 ± 0.1	0.7 ± 0.1	ND[a]	0.9 ± 0.1

[a]The $K_{m,app}$ could not be determined (ND) due to substrate inhibition.

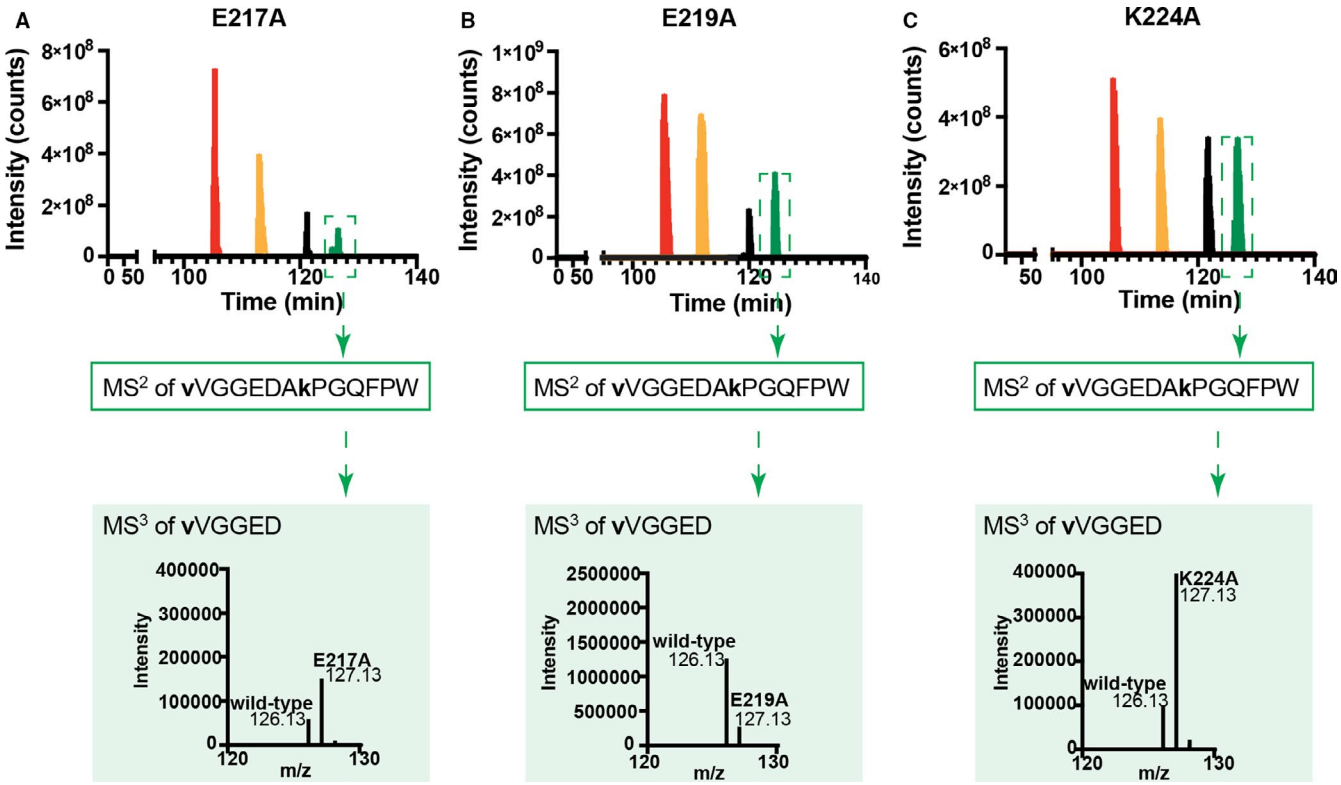

FIGURE 5 Labelling of the N-terminal segment of the protease domain of FIXa variants. TMT-labelling of the N-terminus of (A) FIXaE217A$_{CT}$, (B) FIXaE219A$_{CT}$, and (C) FIXaK224A$_{CT}$. After TMT-labelling and proteolytic digestion, reconstructed ion chromatograms (RICs) were extracted for N-terminal ions VVGGEDAKPGQFPW (red), VVGGEDA**k**PGQFPW (orange), **v**VGGEDAKPGQFPW (black), and **v**VGGEDA**k**PGQFPW (green). These peptides were identified from MS^2 spectra (CID) using Peaks Studio software. Abundance percentages of the fractions with unlabeled Val16$_{CT}$ were estimated and compared with the labelled Val16$_{CT}$ fractions. A representative TMT quantification spectrum is shown for the b6 ion **v**VGGED for each FIXa variant [Color figure can be viewed at wileyonlinelibrary.com]

similar to their enzyme counterparts, except for a few sections that are disordered in the zymogens. These include some specific surface loops that comprise the "activation domain" and the position of the N-terminal section that, once cleaved at the Arg15-Ile16 bond, inserts into the catalytic region and stabilizes the catalytic pocket.[34-36] At the same time, however, it has been recognized that zymogens may display low enzymatic activity toward small substrates and active site-directed inhibitors.[37,38] Since then, numerous studies have provided evidence that the classical distinction between inactive zymogens and active zymogens is no longer tenable. For instance, tissue-type plasminogen activator displays substantial proteolytic activity in its single-chain form, while lacking the novel N-terminus that has been regarded as a hallmark of serine protease activation.[39] Similarly, prothrombin can be activated by binding to the bacterial protein staphylocoagulase, thus providing an example of ligand-induced zymogen activation, independent of limited proteolysis.[31,40] On the other hand, enzymes such as FVIIa and FIXa, despite being processed at the appropriate cleavage sites, display low enzymatic activity in the absence of their cofactors and thus may seem predominantly zymogen-like. More recently, numerous studies

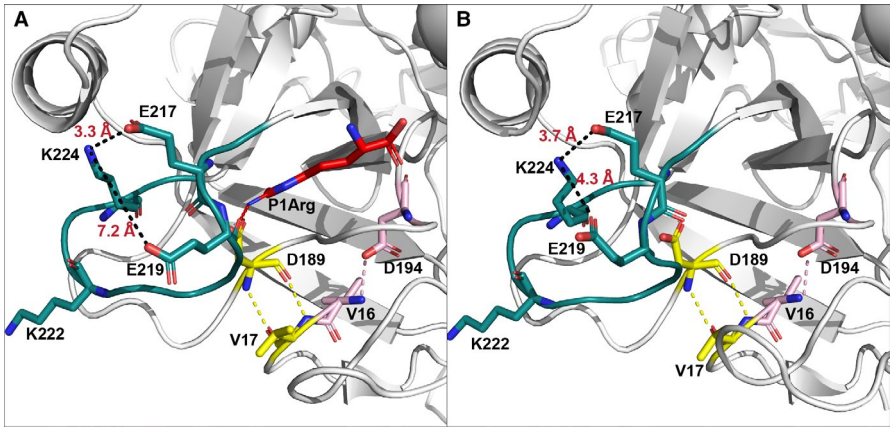

FIGURE 6 Putative network between the 220-loop residues and the N-terminus. (A) Upon occupation of the active site, the interaction of the E219$_{CT}$ carbonyl group with the substrate P1Arg occurs and the distance with K224$_{CT}$ appears to increase (≈7.2 Å, PDB code 2wpm[50]), whereas V17$_{CT}$ in the N-terminal segment pairs with D189$_{CT}$, which takes further contact with the P1Arg. This suggests that the occupation of the S1 pocket drives the substantial interactions that stabilize the active configuration of FIXa. (B) These interactions, however, seem to be missing in absence of a substrate in the S1 pocket and E219$_{CT}$ appears to take a closer contact (distance ≈ 4.3 Å; PDB code 4yzu[51]) with K224$_{CT}$ [Color figure can be viewed at wileyonlinelibrary.com]

addressing the prothrombin/thrombin pair have established that the classical zymogen/enzyme distinction is blurred by the existence of zymogen-like proteases and protease-like zymogens,[23] or, by an equilibrium between closed ("collapsed") and open zymogen (Z* or Z) and enzyme (E* and E) forms.[41]

For the FIX zymogen, no crystal structure is available to facilitate comparison with FIXa. By computational techniques, a model for the zymogen has been derived that predicts a substantial orientational change in the catalytic domain, and the exposure of a largely hydrophobic surface upon release of the activation peptide.[42] In this regard, it seems remarkable that our HDX-MS data indicate that on the backbone level the solution structures of FIX and FIXa are nearly indistinguishable, even in peptides that represent the typical "activation loops,"[23] such as the 140-, 180-, and 220-loops$_{CT}$ (Figures 1, 3 and supporting Figure S2). The few differences that did occur relate to zymogen-specific peptides spanning the scissile bonds at Arg145 and Arg180, and therefore were anticipated (supporting Figure S3). One difference was observed in a peptide from the EGF-2 domain (Figure 1F), wherein the zymogen displayed lower deuterium incorporation. We cannot exclude that FIXa differs from FIX in additional sites in the FIXa light chain, because peptides from the Gla-EGF-1 section were not recovered in our protocol. In this regard, it seems of interest that the activation intermediate FIXα, in which only cleavage at Arg145 has occurred, binds to FVIII, and displays amidolytic activity, despite the Arg180-Val181 scissile bond being intact and the activation peptide still being attached.[26] As such, this FIX derivative may represent an enzyme-like zymogen with the light chain of the FIXa enzyme and the heavy chain of the FIX zymogen. Proteolytic activity, however, remains fully dependent on the cleavage at Arg180 and the generation of the new terminus Val181{16$_{CT}$}.[26] Our present study shows that this cleavage event is accompanied by a reduction in deuterium uptake (Figure 1G) and substantial protection of the N-terminus from labelling (Figure 2).

We previously observed that the 220-loop$_{CT}$ displays reduced deuterium uptake that is not driven by FVIIIa, but by occupancy of the active site.[17] This loop is of particular interest because it is immediately following the region 215 to 217, which is collapsed in the closed Z* and E* conformations and open in enzyme-like Z and E structures.[41] A putative H-bond network herein has been identified that could stabilize the 220-loop$_{CT}$, involving the side chains of E387{217$_{CT}$}, E388{219$_{CT}$}, and Lys394{224$_{CT}$} (Figure 3A).[15] Inspection of 23 available FIXa crystal structures (data not shown) reveals that in all structures the side chains of E387{217$_{CT}$} and Lys394{224$_{CT}$} are sufficiently close (3-4 Å) to support a salt bridge between these two residues. This is supported by our mutagenesis study, which indicates that replacement of either of the two by Ala results in dysfunctional FIXa molecules with an identical phenotype (Figure 4, Table 1). These mutants further displayed an increase in N-terminus labelling (Figure 5), which could be compatible with a more zymogen-like state of these FIXa variants compared with wild-type FIXa. Interestingly, the hemophilia B database contains multiple substitutions in these positions, underlining that disruption of this salt bridge is indeed disease associated.[43]

Together with the 180-loop$_{CT}$, the 220-loop$_{CT}$ comprises a binding site for Na^+, which is coordinated to four backbone carbonyl groups, including the one of Lys394{224$_{CT}$} substituted in our study.[15,44] We considered the possibility that disruption of the H-bond network might affect Na^+-binding and as such could explain reduced FIXa activity. However, the amidolytic activity of neither wild-type FIXa, nor that of the three FIXa mutants displayed any appreciable Na^+-dependence under the conditions tested (Figure S4). Therefore, the functional defect of the FIXa mutants in the 220-loop$_{CT}$ region is not due to altered Na^+-dependence.

Although substitution of E388{219$_{CT}$} resulted in a less severe phenotype, its defect still is compatible with a major role within the 220-loop$_{CT}$ of FIXa (Figure 4; Table 1). Figure 6 shows two examples

from available FIXa structures that indicate that E388{219_{CT}} may not participate in the putative H-bond network that has been identified in the structure of FIXa with *p*-aminobenzamidine in the active site.[15] Instead, in structures containing EGR-derived inhibitors, the backbone carbonyl group of E388{219_{CT}} interacts with the substrate P1Arg, whereas its side chain seems to be pulled away from E387{217_{CT}} (Figure 6A). A similar position of E388{219_{CT}} is seen in the structure of FIXa stabilized by a synthetic inhibitor that binds beyond the active site (Figure 6B). The dysfunction of the E388A{219_{CT}} variant suggests that Ala in this position disturbs the stabilization of the P1Arg-binding pocket, possibly because of a backbone rearrangement within this part of the 220-$loop_{CT}$. It is of interest that, except for FIXa, other serine proteases have Gly in position 219_{CT}, suggesting that this particular S1 site geometry may be unique for FIXa.[45] It seems conceivable that conformational plasticity of the 220-$loop_{CT}$ allows for multiple conformations of E388{219_{CT}} that switch FIXa between free and substrate-bound states during substrate cleavage and subsequent product release, and as such maintains the catalytic cycle.

Substrate-driven changes in FIXa also occur in surface elements other than the 220-$loop_{CT}$, including the 162-$helix_{CT}$ (Figure S2) that is involved in FVIIIa binding.[17] This suggests a critical linkage between this helix and active site occupation, possibly mediated by the disulfide bridge $C168_{CT}$ to $C182_{CT}$.[17] Other substrate-driven changes, including those in peptides from the 140-$loop_{CT}$ and 180-$loop_{CT}$, (Figure 1 and Figure S2) were not further explored because these were also cofactor-driven,[17] and thus considered not predominantly substrate-specific. In our studies, we used the inhibitor EGRck to assess the effect of active site occupation in FIXa. Binding of the natural substrate FX, however, is more complex and probably also involves exosites distant from the active site.[46] Therefore, substrate-driven changes in FIXa may be more extensive than we observed in active-site inhibited FIXa. Further studies could dissect substrate- and cofactor-driven changes in more detail. MS protocols employing further fragmentation of individual peptides into smaller ions should have the potential to analyze such changes at near-residue resolution.

One might question whether related coagulation enzymes display a zymogen-like structure similar to FIXa. In this regard the FVII(a) zymogen/enzyme pair is the best documented example. HDX-MS studies have provided ample evidence that FVIIa retains zymogen-like properties following limited proteolysis, and does not spontaneously rearrange into the active configuration.[16,47] This requires assembly of FVIIa with its cofactor TF, which drives the insertion of the N-terminus into the bottom of the S1-pocket and the rigidification of several surface loops, including the 220-$loop_{CT}$, referred to as activation loop 3.[16] Although our HDX-MS data suggest that FVIIa and FIXa both display an overall zymogen-like structure, there are also differences suggesting that the transition into enzyme in FIXa may be more complex. First, the apparent rigidification at the N-terminus and the 220-$loop_{CT}$, which are driven by TF in FVIIa,[16] are largely EGR-driven in FIXa (Figures 1 and 2) with limited contribution by FVIII.[17] Apparently, full activation of FIXa is driven by both cofactor and substrate. This may also be reflected by the effect of cofactor binding on amidolytic activity: although TF increases FVIIa activity substantially,[48] assembly with FVIIIa has little or no effect on cleavage of peptide substrates by FIXa.[49] Another difference is that in FVIIa the 220-$loop_{CT}$ contains no acidic and basic residues as in FIXa.[16,45] Thus, FVIIa may lack the putative H-bond network, with its concomitant effect on N-terminus insertion in FIXa (Figure 6). A difference in structural plasticity between FVIIa and FIXa in this region may explain why its rigidification is not cofactor-driven in FIXa, but apparently requires occupation of the ArgP1-site by the pseudo-substrate EGR.

Our present data support a picture of two distinct pathways for the allosteric regulation of FIXa: one driven by substrate and another by cofactor binding.[17] The concerted action of both pathways is required to stabilize the zymogen-like FIXa into its active conformation. From a regulatory perspective, it may be beneficial that enzymes in the initial phase of coagulation are zymogen-like, and require further transition into fully competent enzymes. For FIXa function, the dependence on both FVIIIa binding and active site occupation apparently represents a dual barrier. This may serve to limit the risk of premature FX activation, and subsequent amplification thereof downstream in the cascade, thereby reducing the risk of excessive thrombin formation and disruption of the intricate balance between bleeding and thrombosis.

ACKNOWLEDGMENTS

This study has been funded by the Utrecht Institute for Pharmaceutical Sciences (UIPS) and by the Landsteiner Stichting voor Bloedtransfusie Research (LSBR 1417).

CONFLICT OF INTERESTS

None of the authors report any conflict of interest.

AUTHOR CONTRIBUTIONS

Nadia Freato, Alexander B. Meijer, Maartje van den Biggelaar, Koen Mertens, and Eduard H.T.M. Ebberink, designed the study; Nadia Freato, Mariëtte Boon-Spijker, and Eduard H.T.M. Ebberink performed the experimental work; Floris P.J. van Alphen helped with the development of mass spectrometry experiments; Nadia Freato, Alexander B. Meijer, Maartje van den Biggelaar, Koen Mertens, and Eduard H.T.M. Ebberink analyzed and interpreted data; Nadia Freato and Eduard H.T.M. Ebberink made the figures; Nadia Freato, Alexander B. Meijer, Maartje van den Biggelaar, Koen Mertens, and Eduard H.T.M. Ebberink wrote the manuscript.

REFERENCES

1. Davidson C, Hirt R, Lal K, et al. Molecular evolution of the vertebrate blood coagulation network. *Thromb Haemost*. 2003;89:420-428.
2. Davie EW, Fujikawa K, Kisiel W. The coagulation cascade: initiation, maintenance, and regulation. *Biochem*. 1991;30:10363-10370.
3. Page MJ, Di Cera E. Serine peptidases: classification, structure and function. *Cell Mol Life Sci*. 2008;65:1220-1236.
4. Rawlings ND, Barrett AJ. Families of serine peptidases. *Methods Enzymol*. 1994;244:19-61.

5. Hedstrom L. Serine protease mechanism and specificity. *Chem Rev*. 2002;102:4501-4524.
6. Schmidt AE, Bajaj SP. Structure-function relationships in factor IX and factor IXa. *Trends Cardiovasc Med*. 2003;13:39-45.
7. Brandstetter H, Bauer M, Huber R, Lollar P, Bode W. X-ray structure of clotting factor IXa: active site and module structure related to Xase activity and hemophilia B. *Proc Natl Acad Sci U S A*. 1995;92:9796-9800.
8. Hopfner K-P, Lang A, Karcher A, et al. Coagulation factor IXa: the relaxed conformation of Tyr99 blocks substrate binding. *Structure*. 1999;7:989-996.
9. Goettig P, Brandstetter H, Magdolen V. Surface loops of trypsin-like serine proteases as determinants of function. *Biochimie*. 2019;166:52-76.
10. Bjelke JR, Olsen OH, Fodje M, et al. Mechanism of the Ca^{2+}-induced enhancement of the intrinsic factor VIIa activity. *J Biol Chem*. 2008;283:25863-25870.
11. Rezaie AR, Esmon CT. Asp-70–>Lys mutant of factor X lacks high affinity Ca2+ binding site yet retains function. *J Biol Chem*. 1994;269:21495-21499.
12. Mathur A, Zhong D, Sabharwal AK, Smith KJ, Bajaj SP. Interaction of factor IXa with factor VIIIa. Effects of protease domain Ca^{2+} binding site, proteolysis in the autolysis loop, phospholipid, and factor X. *J Biol Chem*. 1997;272:23418-23426.
13. Pineda AO, Carrell CJ, Bush LA, et al. Molecular dissection of Na^{+} binding to thrombin. *J Biol Chem*. 2004;279:31842-31853.
14. Underwood MC, Zhong D, Mathur A, Heyduk T, Bajaj SP. Thermodynamic linkage between the S1 site, the Na^{+} site, and the Ca^{2+} site in the protease domain of human coagulation factor Xa. Studies on catalytic efficiency and inhibitor binding. *J Biol Chem*. 2000;275:36876-36884.
15. Schmidt AE, Stewart JE, Mathur A, Krishnaswamy S, Bajaj SP. Na^{+} site in blood coagulation factor IXa: effect on catalysis and factor VIIIa binding. *J Mol Biol*. 2005;350:78-91.
16. Rand KD, Jørgensen TJD, Olsen OH, et al. Allosteric activation of coagulation factor VIIa visualized by hydrogen exchange. *J Biol Chem*. 2006;281:23018-23024.
17. Freato N, Ebberink EHTM, van Galen J, et al. Factor VIII-driven changes in activated factor IX explored by hydrogen-deuterium exchange mass spectrometry. *Blood*. 2020;136:2703-2714.
18. Mertens K, van Wijngaarden A, Bertina RM. The role of factor VIII in the activation of human blood coagulation factor X by activated factor IX. *Thromb Haemost*. 1985;54:654-660.
19. van Dieijen G, Tans G, Rosing J, Hemker HC. The role of phospholipid and factor VIIIa in the activation of bovine factor X. *J Biol Chem*. 1981;256:3433-3442.
20. Lechtenberg BC, Freund SMV, Huntington JA. An ensemble view of thrombin allostery. *Biol Chem*. 2012;393:889-898.
21. Krishnaswamy S. The transition of prothrombin to thrombin. *J Thromb Haemost*. 2013;11:265-276.
22. Vogt AD, Chakraborty P, Di Cera E. Kinetic dissection of the preexisting conformational equilibrium in the trypsin fold. *J Biol Chem*. 2015;290:22435-22445.
23. Huntington JA. Slow thrombin is zymogen-like. *J Thromb Haemost*. 2009;7:159-164.
24. Fribourg C, Meijer AB, Mertens K. The interface between the EGF2 domain and the protease domain in blood coagulation factor IX contributes to factor VIII binding and factor X activation. *Biochemistry*. 2006;45:10777-10785.
25. Christophe OD, Lenting PJ, Cherel G, et al. Functional mapping of anti-factor IX inhibitors developed in patients with severe hemophilia B. *Blood*. 2001;98:1416-1423.
26. Lenting PJ, Ter Maat H, Clijsters PPFM, Donath MJSH, Van Mourik JA, Mertens K. Cleavage at arginine 145 in human blood coagulation factor IX converts the zymogen into a factor VIII binding enzyme. *J Biol Chem*. 1995;270(25):14884-14890.
27. Bradford MM. A rapid and sensitive method for the quantitation of microgram quantities of protein utilizing the principle of protein-dye binding. *Anal Biochem*. 1976;72:248-254.
28. Meems H, van den Biggelaar M, Rondaij M, van der Zwaan C, Mertens K, Meijer AB. C1 domain residues Lys 2092 and Phe 2093 are of major importance for the endocytic uptake of coagulation factor VIII. *Int J Biochem Cell Biol*. 2011;43:1114-1121.
29. Mertens K, Bertina RM. Activation of human coagulation factor VIII by activated factor X, the common product of the intrinsic and the extrinsic pathway of blood coagulation. *Thromb Haemost*. 1982;47:96-100.
30. Mertens K, Bertina RM. Pathways in the activation of human coagulation factor X. *Biochem J*. 1980;185:647-658.
31. Hendrix H, Lindhout T, Mertens K, Engels W, Hemker HC. Activation of human prothrombin by stoichiometric levels of staphylocoagulase. *J Biol Chem*. 1983;258:3637-3644.
32. Andersen MD, Faber JH. Structural characterization of both the non-proteolytic and proteolytic activation pathways of coagulation factor XIII studied by hydrogen–deuterium exchange mass spectrometry. *Int J Mass Spectrom*. 2011;302:139-148.
33. Bloem E, Ebberink EH, van den Biggelaar M, van der Zwaan C, Mertens K, Meijer AB. A novel chemical footprinting approach identifies critical lysine residues involved in the binding of receptor-associated protein to cluster II of LDL receptor-related protein. *Biochem J*. 2015;468:65-72.
34. Freer ST, Kraut J, Robertus JD, Wright HT, Chymotrypsinogen XNH. 2.5-angstrom crystal structure, comparison with alpha-chymotrypsin, and implications for zymogen activation. *Biochemistry*. 1970;9:1997-2009.
35. Bode W, Huber R. Induction of the bovine trypsinogen-trypsin transition by peptides sequentially similar to the N-terminus of trypsin. *FEBS Lett*. 1976;68:231-236.
36. Bode W, Schwager P, Huber R. The transition of bovine trypsinogen to a trypsin-like state upon strong ligand binding. *J Mol Biol*. 1978;118:99-112.
37. Morgan PH, Robinson NC, Walsh KA, Neurath H. Inactivation of bovine trypsinogen and chymotrypsinogen by diisopropylphosphorofluoridate. *Proc Natl Acad Sci U S A*. 1972;69:3312-3316.
38. Neurath H, Walsh KA. Role of proteolytic enzymes in biological regulation (a review). *Proc Natl Acad Sci U S A*. 1976;73:3825-3832.
39. Rijken DC, Hoylaerts M, Collen D. Fibrinolytic properties of one-chain and two-chain human extrinsic (tissue-type) plasminogen activator. *J Biol Chem*. 1982;257(6):2920-2925.
40. Friedrich R, Panizzi P, Fuentes-Prior P, et al. Staphylocoagulase is a prototype for the mechanism of cofactor-induced zymogen activation. *Nature*. 2003;425:535-539.
41. Gohara DW, Di Cera E. Allostery in trypsin-like proteases suggests new therapeutic strategies. *Trends Biotechnol*. 2011;29:577-585.
42. Perera L, Darden TA, Pedersen LG. Modeling human zymogen factor IX. *Thromb Haemost*. 2001;85:596-603.
43. Rallapalli PM, Kemball-Cook G, Tuddenham EG, Gomez K, Perkins SJ. An interactive mutation database for human coagulation factor IX provides novel insights into the phenotypes and genetics of hemophilia B. *J Thromb Haemost*. 2013;11:1329-1340.
44. Vadivel K, Schreuder HA, Liesum A, Schmidt AE, Goldsmith G, Bajaj SP. Sodium-site in serine protease domain of human coagulation factor IXa: evidence from the crystal structure and molecular dynamics simulations study. *J Thromb Haemost*. 2019;17:574-584.
45. Hopfner KP, Brandstetter H, Karcher A, et al. Converting blood coagulation factor IXa into factor Xa: dramatic increase in amidolytic activity identifies important active site determinants. *EMBO J*. 1997;16:6626-6635.
46. Basavaraj MG, Krishnaswamy S. Exosite binding drives substrate affinity for the activation of coagulation factor X by the intrinsic Xase complex. *J Biol Chem*. 2020;295:15198-15207.

47. Song H, Olsen OH, Persson E, Rand KD. Sites involved in intra- and interdomain allostery associated with the activation of factor VIIa pinpointed by hydrogen-deuterium exchange and electron transfer dissociation mass spectrometry. *J Biol Chem*. 2014;289:35388-35396.
48. Krishnaswamy S. The interaction of human factor VIIa with tissue factor. *J Biol Chem*. 1992;267:23696-23706.
49. Hsu YC, Hamaguchi N, Chang YJ, Lin SW. The distinct roles that Gln-192 and Glu-217 of factor IX play in selectivity for macromolecular substrates and inhibitors. *Biochemistry*. 2001;40:11261-11269.
50. Zogg T, Brandstetter H. Structural basis of the cofactor- and substrate-assisted activation of human coagulation factor IXa. *Structure*. 2009;17:1669-1678.
51. Parker DL, Walsh S, Li B, et al. Rapid development of two factor IXa inhibitors from hit to lead. *Bioorg Med Chem Lett*. 2015;25:2321-2325.

SUPPORTING INFORMATION

Additional supporting information may be found online in the Supporting Information section.

How to cite this article: Freato N, van Alphen FP, Boon-Spijker M, et al. Probing activation-driven changes in coagulation factor IX by mass spectrometry. *J Thromb Haemost*. 2021;19:1447–1459. https://doi.org/10.1111/jth.15288